IEEE Access
Multidisciplinary | Rapid Review | Open Access Journal

Received April 8, 2019, accepted April 22, 2019, date of publication April 29, 2019, date of current version May 28, 2019.

Digital Object Identifier 10.1109/ACCESS.2019.2913671

Geophysical Potential Field Anomaly Separation Method With Optimal Mother Wavelet and Spatial Locating Multiresolution Analysis (MRA)

CAI-YUN LIU[1], CHANG-LI YAO[2], AND JIE XIONG[3]
[1]School of Mathematics and Information, Yangtze University, Jingzhou 434023, China
[2]School of Geophysics and Information Technology, China University of Geosciences, Beijing 100083, China
[3]School of Electronics and Information, Yangtze University, Jingzhou 434023, China

Corresponding author: Cai-Yun Liu (liucaiyun01@yangtzeu.edu.cn)

This work was supported in part by the National Natural Science Foundation of China under Grant 61673006 and Grant 61273179, in part by the Project of Educational Commission of Hubei Province of China under Grant B2016034, and in part by the Research Project of University Laboratory Work of Hubei Province of China under Grant HBSY2017-04.

ABSTRACT Gravity or magnetic field, say geophysical potential field, is the superposition of gravity or magnetic effects of all geological bodies of different depths, scales, and forms. The signal, say anomaly, caused by the target geological body must be separated from the measured potential field before used for inversion and interpretation. The classical separation methods based on multiresolution analysis (MRA) have two problems. One is how to choose the optimal mother wavelet to separate the anomalies. Another is how to separate the anomalies better when the spectrum of different geological bodies aliased each other in scale. For the first problem, we propose a quantitative evaluating indicator, sparse index (SI), to help us choose the optimal mother wavelet for the particular separation task. For the second problem, we separate the residual anomalies based on MRA with spatial locating, using the wavelet coefficients within particular spatial and scale arrange to reconstruct the regional and residual anomaly, respectively. The results of three experiments, including separating the magnetic anomalies of a 2D and a 3D geology model, show that our new approach combining optimal mother wavelet and spatial locating MRA separation is superior to the classical wavelet transform method and can improve the accuracy of separation result obviously.

INDEX TERMS Localized separation, multiresolution analysis (MRA), potential anomaly separation, quantitative evaluating of mother wavelet, sparse index (SI).

I. INTRODUCTION

Investigations of terrestrial gravity and magnetic fields, say geophysical potential field, are among the oldest methods for determining the nature and processes of Earth [1]. The gravity and magnetic methods continue to have an important, often decisive role, in a wide variety of terrestrial investigations, mineral and hydrocarbon resources exploration [1]–[3]. Gravity or magnetic potential field anomalies are the superposition of the gravity or magnetic effects of all geological bodies of different depths, scales, and forms. To invert a particular geological body from the measured potential field anomaly, the anomaly caused by the target geological body must be separated before used for inversion and interpretation [4]. Typically, the total potential field anomaly is separated into the regional anomaly, caused by deeper and larger geological bodies, and the residual anomaly, caused by shallower and smaller ones. Due to the inherent non-uniqueness of geophysical potential field, the separation of the potential field anomaly is one of the difficulties in the processing and interpretation of the geophysical potential field data.

There are many methods for the separation of the potential field anomaly [4], including the least squares smoothing method [3], the analytical continuation method [3], the trend analysis method [3], the matching filtering method [5], the Wiener filtering method [6], the nonlinear filtering method [7], the preferential filtering method [8], and wavelet preferential spatially varying filtering method [4]. These methods have their own characteristics and advantages, but they also have some limitations [4].

The associate editor coordinating the review of this manuscript and approving it for publication was Filbert Juwono.

Wavelet transform is a widely concerned digital signal processing method [9]–[11]. Because of its good local analysis ability in both spatial and frequency domains, it is usually used to analyze signals with transient, unsteady or time-varying characteristics. Among them, Mallat proposed the theory of MRA based on discrete wavelet transform, and established the Mallat algorithm of wavelet decomposition and reconstruction [12]. In recent years, many scholars have carried out research on potential field anomaly separation based on MRA, and achieved remarkable results [13]–[18]. The core ideas of these methods are decomposing the potential field anomaly at multiresolution, firstly; determining the corresponding scale ranges of regional anomaly and residual anomaly, respectively, secondly; using the wavelet coefficients in the particular scale ranges to reconstruct regional and residual anomaly respectively, lastly. There is no different between classical MRA separation methods and frequency domain separation methods, but using different basis functions (wavelet function, or sine basis function).

The classical MRA separation methods mentioned above have two problems. On the one hand, it is still an open issue about how to choose the best mother wavelet for the particular separation task, since different mother wavelets have a great impact on the separation results [19]. On the other hand, there is the incomplete separation problem when wavelet spectrum of regional and residual anomalies aliased each other in the scale, since the classical methods did not make use of the spatial information of wavelet transform.

In order to deal with the two problems mentioned above, we propose a quantitative evaluation factor, sparse index, to help us choose the best mother wavelet, firstly; then we propose a separation method based on MRA with spatial locating, which reconstruct the regional and residual anomalies by using the wavelet coefficients within particular spatial and scale arrange, respectively; and we test our new approach with three experiments, including magnetic anomalies separation of a 2D and a 3D geology model, lastly.

II. METHODOLOGY

A. CLASSICAL SEPARATION METHOD BASED ON MRA

1) WAVELET TRANSFORM

For any signal $s(x) \in L^2(R)$, its continuous wavelet transform is defined as [20], [21]

$$W_{g|s}(a,b) = \frac{1}{\sqrt{a}} \int_{-\infty}^{\infty} s(x) g^* \left(\frac{x-b}{a} \right) dx, \tag{1}$$

where $g(x)$ is the mother wavelet, $g^*(x)$ is the complex conjugate of $g(x)$. The transformed signal $W_{g|s}(a,b)$ is a function of the scale a and translation b.

In the case of discrete transform, discrete values are used for a, b, the commonest choice being a dyadic grid, i.e. $a = 2^j, b = kb_0 2^j$, where b_0 is a constant. The discrete wavelet transform may therefore be more conveniently written as

$$d_j(k) = W_{g|s}(j,k) = \int_{-\infty}^{\infty} s(x) g^*_{j,k}(x) dx, \tag{2}$$

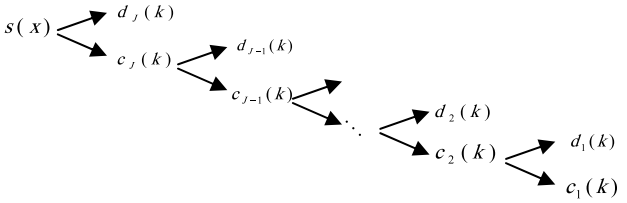

FIGURE 1. Pyramid architecture of the MRA algorithm. The final decomposition consists of a low-resolution approximation (approximation coefficient) and a set of details (detail coefficient) of signal.

with

$$g_{j,k}(x) = \frac{1}{\sqrt{2^j}} g\left(\frac{x - kb_0 2^j}{2^j} \right) dx, \quad j,k \in Z. \tag{3}$$

The original signal $s(x)$ can be synthesized by the inversion discrete wavelet transform:

$$s(x) = \sum_{j=0}^{\infty} \sum_{k=-\infty}^{\infty} d_j(k) \tilde{g}_{j,k}(x). \tag{4}$$

2) MULTIRESOLUTIONAL ANALYSIS (MRA)

Discrete wavelets are functions that form basis for the functional space $L^2(R)$, the space of all functions for which the integral of the square of its absolute value taken over time interval $(-\infty, \infty)$. The wavelet basis for $L^2(R)$ actually is a dual basis consisting of a pair of basis window functions known as the scaling function and the wavelet function respectively [21]. This functional pair partitions the space $L^2(R)$ into a decomposition that has a special algebraic structure, which is known as a MRA of $L^2(R)$. Both the scaling function, $\phi(x)$, and the wavelet function, $g(x)$, generate a sequence of subspace, $\{V_j\}$ by the scaling function, and $\{W_j\}$, by the wavelet function, whose union generates $L^2(R)$ as $j \to \infty$.

$$L^2(R) = V_1 \oplus W_1 \oplus W_2 \oplus W_3 \oplus \ldots W_j, \quad j \to \infty \tag{5}$$

$$V_{j+1} = V_j \oplus W_j \tag{6}$$

Any signal $s(x) \in L^2(R)$could be decomposed as following:

$$s(x) = \sum_k c_1(k) \varphi_{1,k}(x) + \sum_k \sum_{j=1}^{J} d_j(k) g_{j,k}(x), \tag{7}$$

where $c_1(k)$is scaling coefficient (approximation coefficient), $d_j(k)$ is wavelet coefficient (detail coefficient), $\varphi_{1,k}(t)$is scaling function, $g_{j,k}(x)$is wavelet function.

We summarize the whole MRA process in Figure 1.

3) CLASSICAL SEPARATION METHOD BASED ON MRA

The classical separation method based on MRA, for the geophysical potential field anomalies, is decomposing potential field data into first-order approximation coefficient, $c_1(k)$, and several detail coefficients, $d_j(k)$; then reconstructing the regional and residual anomalies using particular

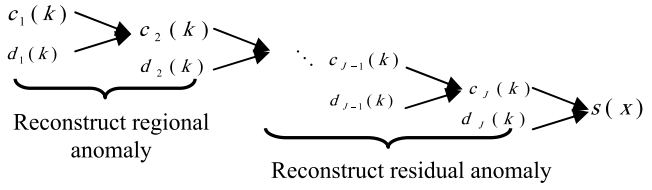

FIGURE 2. Classical separation method for geophysical potential field anomaly based on MRA.

range of wavelet coefficients, respectively. For example, the regional anomalies are reconstructed from first-order approximation coefficient $c_1(k)$, first-order detail coefficient $d_1(k)$, and second-order coefficient $d_2(k)$; while the residual anomalies are constructed from the rest wavelet coefficient $d_3(k), \ldots, d_{J-1}(k), d_J(k)$. The classical separation method based on MRA is illustrated in Figure 2.

On the one hand, it is still an open issue about how to choose the best mother wavelet for separation, since different mother wavelets have a great impact on the separation results [19]. On the other hand, the classical separation method performs anomalies separation only on the scale domain, which means all the wavelet coefficients belonging to one scale is used to reconstruct whether regional or residual anomalies. When the regional and residual anomalies are aliased in scale domain (that is, the wavelet coefficients of a certain scale contain both residual anomaly components and regional anomaly components), there is still the problem of incomplete separation (see the results of Section 3.2 Separation experiment for the 2D model for the detail). We propose an optimal mother wavelet choosing method and a spatial locating MRA separation to address these problems.

B. OUR APPROACH

1) OPTIMAL MOTHER WAVELET

The main challenge in using wavelet transform is selecting the optimal mother wavelet for the given tasks, as different mother wavelet applied to the same signal may produce different results [22]–[24]. In order to avoid the subjectivity of choosing mother wavelet for the anomaly separation, we need a quantitative evaluation index for choosing an optimal mother wavelet.

The signal is represented as a set of wavelet coefficients, after wavelet transform, in the spatial-scale domain. Generally speaking, only a small number of wavelet coefficients' absolute value are significantly large, while the rest coefficients' absolute value are small, or even close or equal to zero. As we mentioned above, the aliasing of regional and residual anomalies in scale domain will lead to the problem of incomplete separation. The more of zero wavelet coefficients obtained after wavelet transform (say more sparse), the lower the probability of aliasing in scale domain will occur, so that the better separation results could be expected.

Follow the idea mentioned above, we introduce a quantitative evaluation index for choosing an optimal mother wavelet, say Sparse Index (SI), as follow:

$$SI = \sum_j \sum_k \frac{\left\|W_{gs}(j,k)\right\|^2}{\left\|W_{gs}(j,k)\right\|^2 + \varepsilon}, \tag{8}$$

where $W_{g|s}(j,k)$ is the wavelet coefficients of scale j and spatial position k,ε is an infinitesimal constants, such as $\varepsilon = 10^{-8}$.

If $W_{g|s}(j,k) = 0$, $SI = \frac{\|W_{g|s}(j,k)\|^2}{\|W_{g|s}(j,k)\|^2+\varepsilon} = 0$; else if $W_{g|s}(j,k) \neq 0$, $SI = \frac{\|W_{g|s}(j,k)\|^2}{\|W_{g|s}(j,k)\|^2+\varepsilon} = 1$. SI is the number of non-zero wavelet coefficients, which indicates the sparsity of the wavelet coefficients. The smaller SI is, the lower probability of aliasing in scale domain will occur, so that the better separation results will be obtain.

2) SEPARATION WITH OPTIMAL MOTHER WAVELET AND SPATIAL LOCATING MRA

Choosing the optimal mother wavelet using SI could sparse the wavelet coefficients and alleviate the aliasing degree of regional and residual anomalies in scale domain. However, separating the regional and residual anomalies only in scale domain may be incompletely, since the aliasing may still exist in scale domain, see Figure 10 as an example, in which the regional and residual anomalies aliasing in 5th order detail coefficients, even using optimal mother wavelet. In fact, the wavelet coefficients contain not only the scale information, but also spatial position information. We could make use of these spatial position information to improve the accuracy of separation. Taking the Figure 10 as an example, again, we may reconstruct the residual anomaly only using the detail coefficients limited in the red box. We name this method as spatial locating MRA because only the certain detail coefficients in spatial range, say normalized horizontal position from 0.7 to 0.8 in Figure 10, are used to reconstruct the residual anomaly. The spatial locating MRA could improve the separating result when the residual and regional anomalies aliasing in the 5th order detail coefficients, because we ignore the coefficients outside red box that corresponding to the regional anomaly when we reconstruct the residual anomaly.

Followed the idea discussed above, the separation method with optimal mother wavelet and spatial locating MRA is described as follows:

Step 1: Choose the optimal mother wavelet by SI factor;

Step 2: Decompose the potential field with MRA, obtaining the approximation coefficients and detail coefficients;

Step 3: Determine the range of coefficients of residual anomaly, say R, in scale-spatial domain (taking the Figure 10 as an example, again, R is the area limited in the red box), according the local distribution characteristics of residual anomaly;

Step 4: Reconstruct the residual anomaly using the detail coefficients limited in the range R;

Step 5: Reconstruct the regional anomaly using the approximation coefficients and the rest detail coefficients.

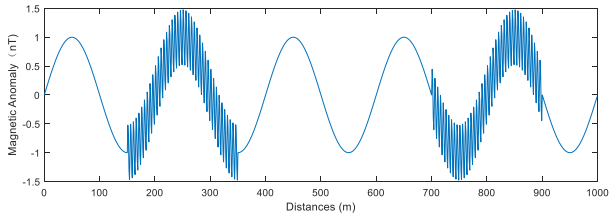

FIGURE 3. Waveform of signal, which consists two frequency sinusoidal component, say 0.005 circles/m and 0.2 circles/m.

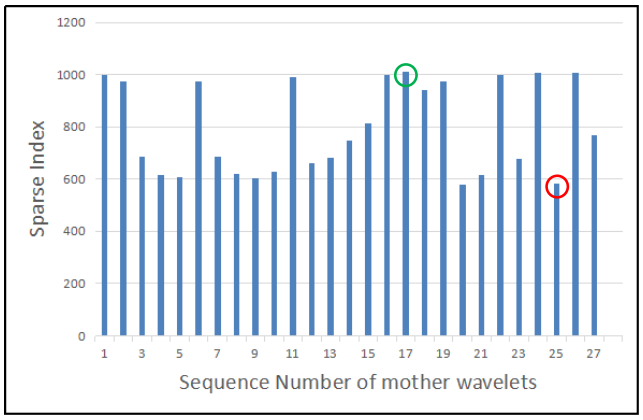

FIGURE 4. The factor SI of the signal y using different mother wavelets.

TABLE 1. Names and sequence numbers of different mother wavelets.

Seq. No.	Mother Wavelet	Seq. No.	Mother Wavelet	Seq. No.	Mother Wavelet	Seq. No.	Mother Wavelet
1	db1	8	sym4	15	coif5	22	rbio1.1
2	db2	9	sym5	16	bior1.1	23	rbio1.3
3	db3	10	sym6	17	bior1.3	24	rbio2.2
4	db4	11	coif1	18	bior2.2	25	rbio2.4
5	db5	12	coif2	19	bior2.4	26	rbio3.1
6	sym2	13	coif3	20	bior3.1	27	rbio3.3
7	sym3	14	coif4	21	bior3.3		

III. RESULTS

A. SEPARATION EXPERIMENT FOR THE SIMPLE SINUSOIDAL SIGNALS

The factor of SI could help us to choose an optimal mother wavelet for signal separation. We use the following signal, shown in Figure 3, as an example to demonstrate the role of SI in the separation.

$$y = \begin{cases} \sin(2\pi f_1 x) + 0.5 * \sin(2\pi f_2 x), & x \in [150, 350] \ or \\ \qquad\qquad x \in [700, 900] \\ \sin(2\pi f_1 x), & otherwise \end{cases} \tag{9}$$

where $f_1 = 0.005 circles * m^{-1}, f_2 = 0.2 circles \cdot m^{-1}$.

In order to choose an optimal mother wavelet, we calculate the SI, according to formulate (8) of signal y using different mother wavelets listed in Table 1, respectively. Then we show the results in Figure 4.

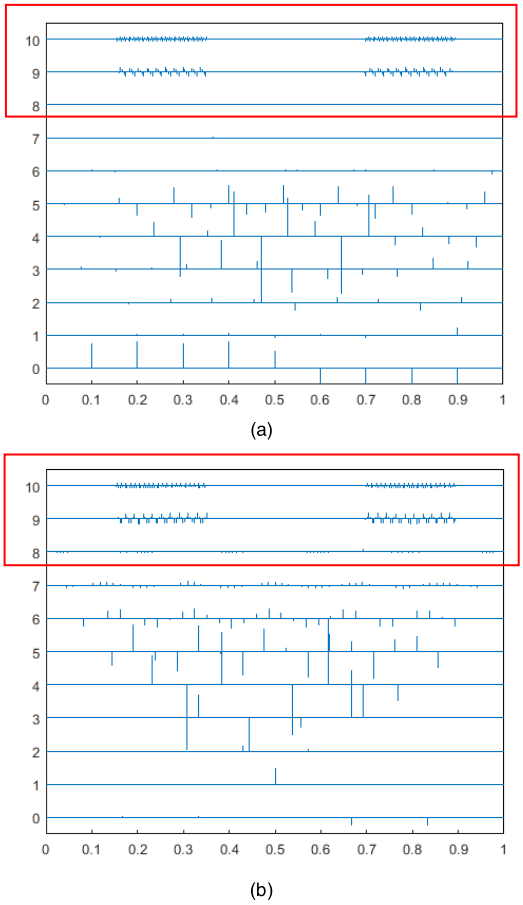

FIGURE 5. The wavelet coefficients of MRA of signal with the best mother wavelet rbio2.4 (a) and the worst one bior1.3 (b).

From the Figure 4 we can see that the best mother wavelet is no. 25 (rbio2.4), indicated with red circle, while the worst one is no. 17 (bior1.3), indicated with green circle.

The wavelet coefficients of MRA of signal y with the best mother wavelet rbio2.4, and the worst one bior1.3 are shown in Figure 5 (a), (b) respectively. Figure 5 compose several rows of pulse. Each row of pulses represents the wavelet coefficients at a certain scale. The first order approximation coefficients are represented by the row of pulses with 0 ordinates, and the $1^{st}-9^{th}$ order detail coefficients are represented by rows with 1 to 9 ordinates, respectively. The height of each pulse represents the value of coefficient, and the abscissa in the figure is the normalized horizontal position.

From Figure 5 we can see that the $8^{th} - 10^{th}$ order detail coefficients represents the higher frequency components of signal $y(0.2\ circles \cdot m^{-1})$, while the rest of detail and approximation coefficients represent the lower frequency component of signal y $(0.05 circles \cdot m^{-1})$. We zoom in the red rectangle part of Figure 5, and show it in Figure 6, respectively. From Figure 6 (a) we can see the best mother wavelet rbio2.4 separates the higher frequency component of signal y pretty well. However, from Figure 6(b) we can see that the worst mother wavelet bior1.3 separates the higher frequency component incompletely. The higher frequency components (limited in

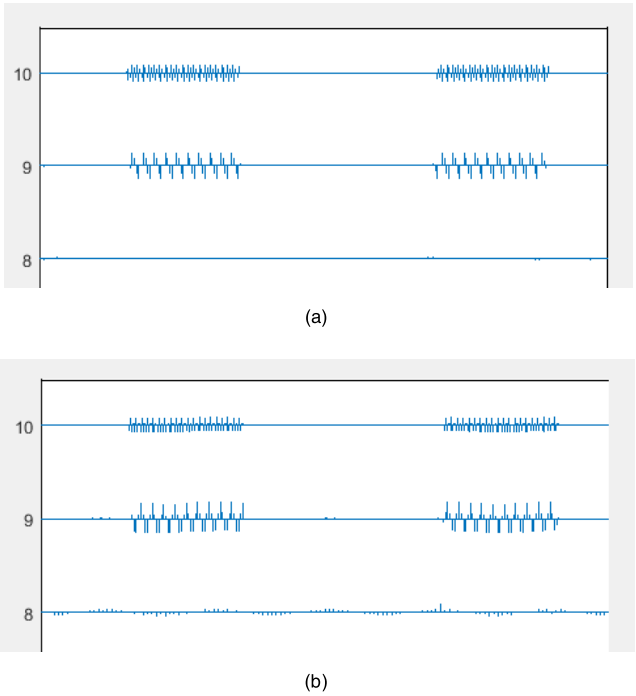

FIGURE 6. Zoom in the red rectangle part of Figure 5(a) and (b), respectively.

green box) aliased by the lower ones (spread in the whole 8^{th} row) in the 8^{th} order detail coefficients.

The separation results of signal y using the worst mother wavelet bior1.3 are shown in Figure 7. From Figure 7 (b) we can see that the separated higher frequency components contain some lower frequency ones, while the separated lower components become jugged.

The separation results of signal y using the best mother wavelet rbio2.4 are shown in Figure 8. From Figure 8 (b) we can see that the separated higher frequency components are more clear, and the separated lower components become much more smooth.

Comparing the results of Figure 7 and Figure 8, we can see that using best mother wavelet chosen by SI factor, we could separate higher and lower frequency components from the signal more clearly.

B. SEPARATION EXPERIMENT FOR THE 2D MODEL

The experiment discussed above is just to separate the simple sinusoidal signals. We will consider a 2D geological bodies model and separate its magnetic anomalies into regional and residual anomalies.

Model 1: This is a 2D geological bodies model which consists of two horizontal infinite extension cylinders underground. For the cylinder 1, depth = 3000m, radius = 300m, horizontal position = 5000m, vertical magnetization = 1A/m; for the cylinder 2, depth = 50m, radius = 30m, horizontal position = 8000m, vertical magnetization = 0.06A/m. The parameters of the model 1 are listed in Table 2.

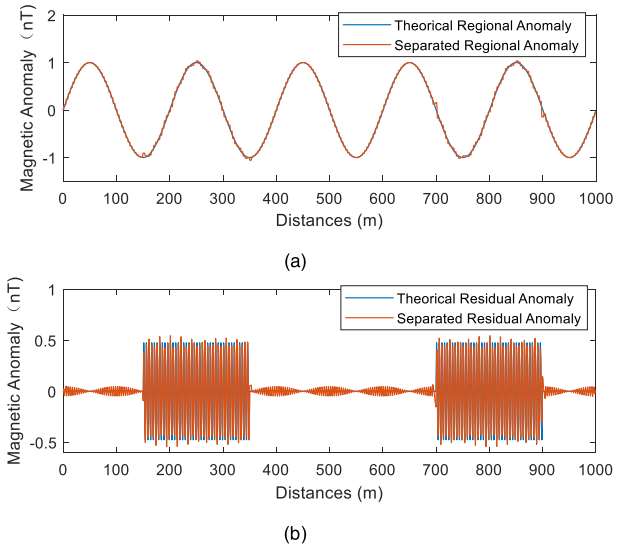

FIGURE 7. The separation results of signal y using the worst mother wavelet bior1.3. (a) Separated lower frequency components (regional anomaly). (b) Separated higher frequency components (residual anomaly).

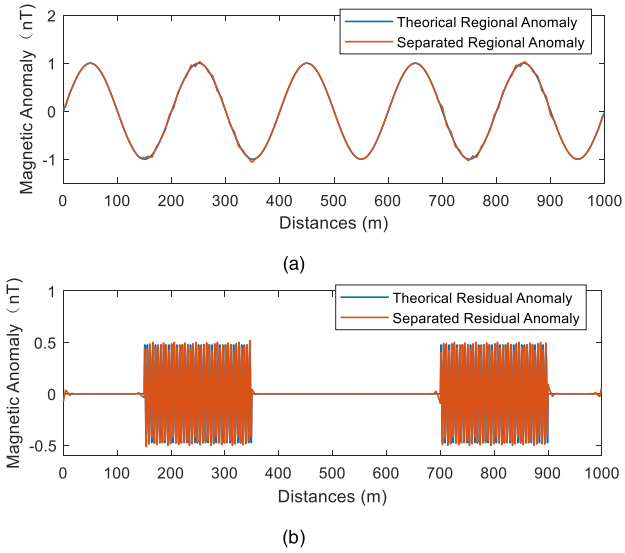

FIGURE 8. The separation results of signal y using the best mother wavelet rbio2.4. (a) Separated lower frequency components (regional anomaly). (b) Separated higher frequency components (residual anomaly).

TABLE 2. Parameters of model 1 (2D geological bodies model of two horizontal infinite extension cylinders).

Model	Depth (m)	Position (m)	Radius (m)	Magnetization (A/m)
cylinder 1	3000	5000	300	1
cylinder 2	50	8000	30	0.06

The observation profile length is 10,00m on the ground, and the observation interval is 10m. The observed magnetic anomaly of model 1 are shown in Figure 9.

The magnetic anomaly is decomposed in multi-scale with 'db2' mother wavelet. The wavelet coefficients are shown

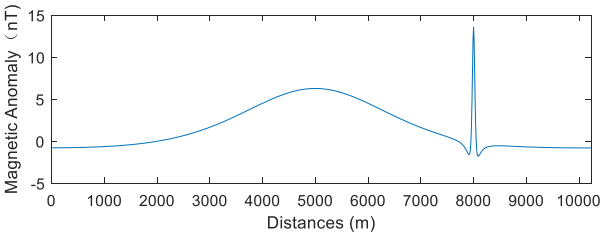

FIGURE 9. The magnetic anomaly of model 1.

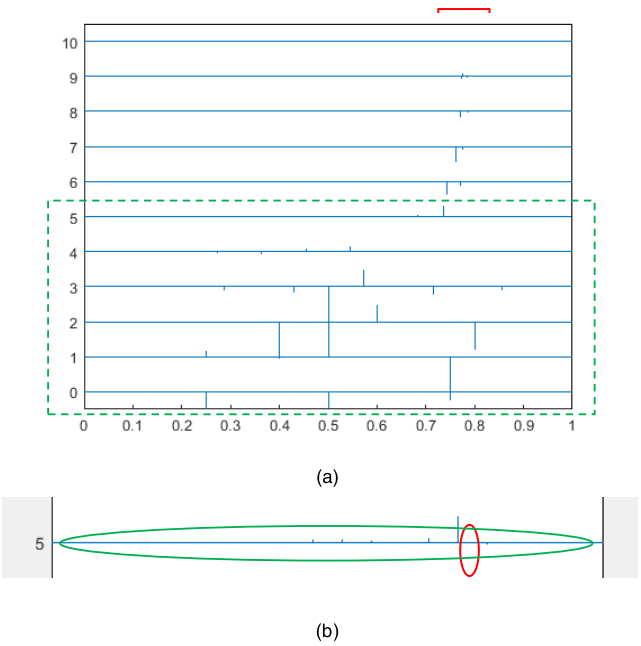

FIGURE 10. Multiscale decomposition wavelet coefficients of magnetic anomaly of model 1. (a) Marking the residual and regional anomalies; (b) zoom in 5th order detail coefficients to show the aliasing of residual and regional anomaly, coefficients in red ellipses corresponding to the residual anomaly, while those in green one corresponding to the regional anomaly.

in Figure 10. We mark out the coefficients of residual anomaly with red box and coefficients of regional anomaly in green dashed box, see Figure 10(a). The residual and regional anomaly aliasing in scale 5, which can be seen clearly in Figure 10 (b).

From Figure. 10, it can be seen that the $5^{th}-9^{th}$ order detail coefficients have significant amplitudes near the abscissa, indicating that there is a high frequency signal nearby (residual anomaly); in addition, the $1^{st}-5^{th}$ order detail coefficients and the 1^{st} order approximation coefficients have significant global amplitudes, indicating that there is a large-scale global signal (regional anomaly). Because of the residual anomaly and regional anomaly aliasing on the 5^{th}order detail coefficient (see Figure 10b for the detail), it can be predicted that the residual and regional anomalies can not be completely separated from total magnetic anomaly on the scale alone.

According to the above analysis, the residual anomaly is reconstructed by $5^{th}-10^{th}$ order detail coefficients, and the

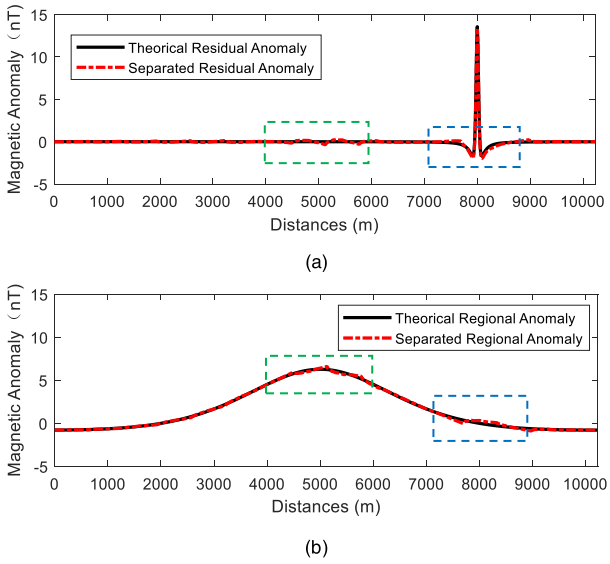

FIGURE 11. Separation result of magnetic anomaly of model 1 as: (a) using $5^{th}-10^{th}$ order detail coefficients to reconstruct residual anomaly; (b) using rest of coefficients to reconstruct regional anomaly.

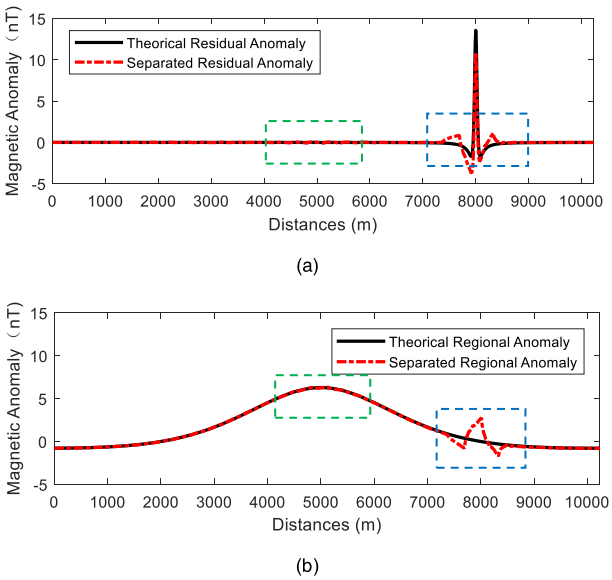

FIGURE 12. Separation result of magnetic anomaly of model 1 as: (a) using $6^{th}-10^{th}$ order detail coefficients to reconstruct residual anomaly; (b) using rest of coefficients to reconstruct regional anomaly.

regional anomaly is reconstructed by the rest coefficients. The separation results are shown in Figure 11. We can see, from Figure 11, that the reconstructed residual anomaly contains part of the regional anomaly information (see the green dashed boxes in Figure 11a). Correspondingly, the result of regional anomaly separation appears more obvious jagged phenomenon (see the green and blue dashed boxes in Figure 11b). The reason of incomplete separation is that the 5^{th} order detail coefficients contain the information not only of regional anomaly but of residual one.

If we reconstruct the residual anomaly only by 6^{th} -9^{th} order detail coefficients and reconstruct the regional anomaly

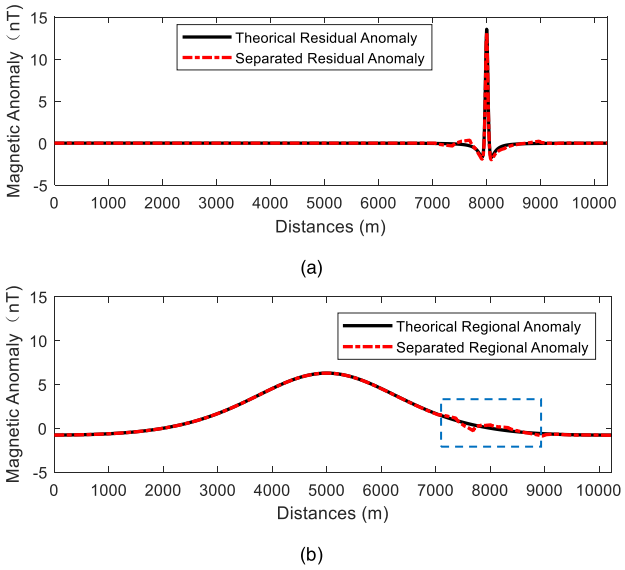

FIGURE 13. Separation result of magnetic anomaly of model 1 with spatial locating as: (a) using $6^{th}-10^{th}$ order detail coefficients in the red box in Figure 10a to reconstruct residual anomaly; (b) using rest of coefficients to reconstruct regional anomaly.

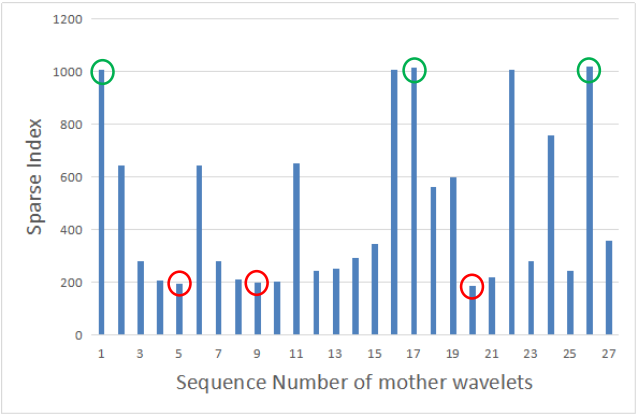

FIGURE 14. The factor SI of the magnetic anomaly of model 1 using different mother wavelets.

by the rest coefficients, the separation results are still incomplete as shown in Figure 12. As can be seen from Figure. 12, the reconstructed residual anomaly loses part of the information (its amplitude is attenuated), and the missing part is separated into the regional anomaly. Some of the aliasing phenomenon have been improved (see the green dashed boxes in Figure 12a,b), but some of aliasing becomes worse (see the blue dashed box near by $x = 8000m$in Figure 12a, b).

Comparing the separation results of Figure. 11 and Figure. 12, it can be seen that the separation result of classical MRA method is not ideal when there is aliasing of regional and residual anomaly on scale (for example, in this case, there is aliasing of regional and residual anomaly on the 5^{th} order detail coefficients).

If we utilized the spatial information of wavelet transform, we will obtain a better separation result by using the wavelet

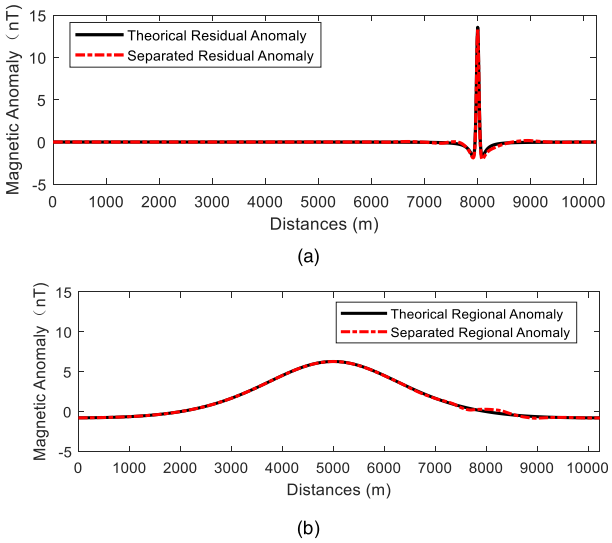

FIGURE 15. Separation result of magnetic anomaly of model 1 with spatial locating MRA and optimal mother wavelet, say 'sym5', as: (a) using $6^{th}-10^{th}$ order detail coefficients in the red box in Figure 10(a) to reconstruct residual anomaly; (b) using rest of coefficients to reconstruct regional anomaly.

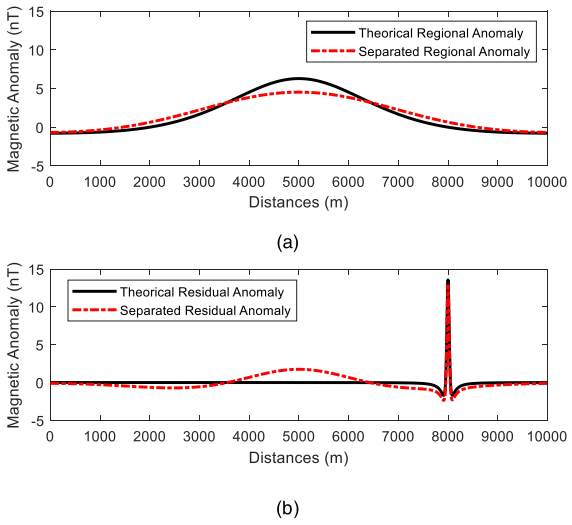

FIGURE 16. Separation result of magnetic anomaly of model 1 of frequency filtering with 2/L cut-off frequency as: (a) low-pass filtering result, say regional anomaly; (b) high-pass filtering result, say residual anomaly. L = 10000m is the length of profile and data interval is 10m.

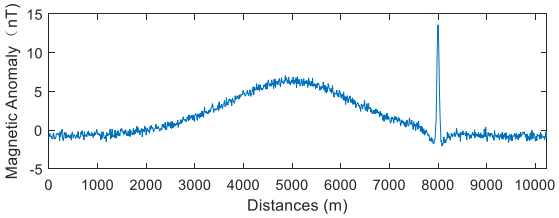

FIGURE 17. The magnetic anomaly of model 1 with 10 db Gaussian white noise.

coefficients in the red box in the Figure 10(a) to reconstruct residual anomaly and using the rest ones to reconstruct the regional anomaly. In this way, we can make full use of all

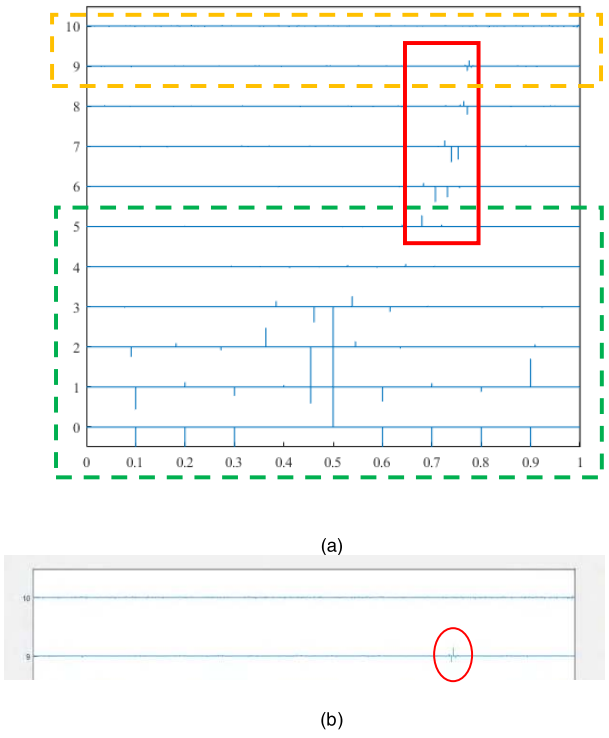

FIGURE 18. Multiscale decomposition wavelet coefficients of magnetic anomaly of model 1 with 10 db Gaussian white noise. (a) Marking the residual, regional anomalies, and noise; (b) zoom in 9^{th} and 10^{th} order detail coefficients to show the aliasing of residual anomaly and noise, coefficients in red ellipses corresponding to the residual anomaly, while the rest coefficients corresponding to the noise.

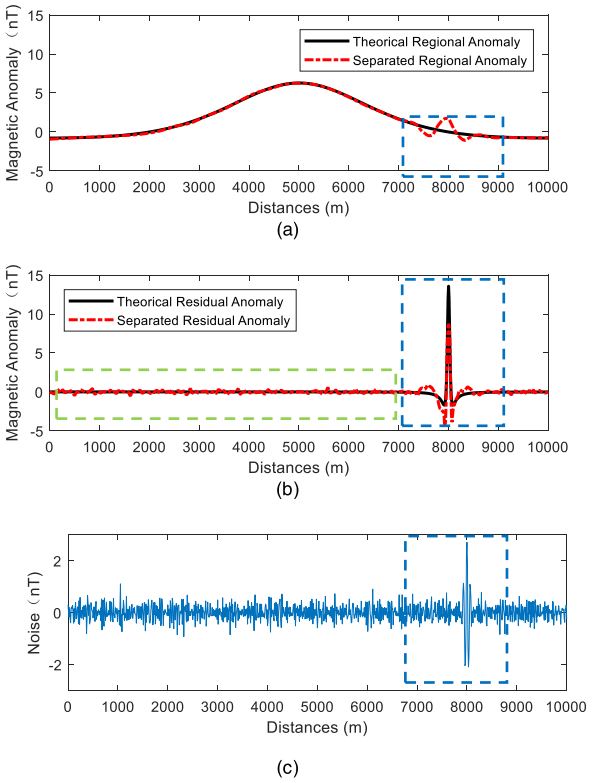

FIGURE 19. Separation result of magnetic anomaly of model 1 as: (a) using 6^{th} -8^{th} order detail coefficients to reconstruct residual anomaly; (b) using rest of coefficients to reconstruct regional anomaly; (c) using 9^{th} -10^{th} order detail coefficients to reconstruct noise.

the detail coefficients corresponding to the residual anomaly (5^{th} – 10^{th} order details), and avoid the interference of regional anomaly in the 5^{th} order details, so as to achieve precise locating and separation. The separation results are shown in Figure 13.

From Figure 13 we can see that the residual and regional anomaly are separated more accurately by using the spatial locating MRA separation method, and the separation results are basically consistent with the theoretical values. It is worth pointing out that there is still a small step phenomenon near by $x = 8000m$(see blue dashed box in Figure 13b), which is consistent with the location of the residual anomaly (corresponding to the shallower cylinder 2).

We could alleviate the step phenomenon in Figure 13 by choosing the optimal mother wavelet with SI factor. For model 1 magnetic anomalies, a set of mother wavelets (see Table 1) are selected to calculate their corresponding SI, and the results are shown in Figure 14.

As can be seen from Figure 14, the three best mother wavelets are 'db5', 'sym5' and 'bior3.1' (mother wavelets numbered 5, 9 and 20 in the red circle). The three worst mother wavelets are 'rbio3.1', 'bior1.3' and 'db1' (mother wavelets numbered 26, 17 and 1 in the green circle).

The spatial locating MRA separation and the optimal mother wavelet 'sym5' are employed to separate the magnetic anomalies. The separation results are shown in Figure 15. From Figure 15, it can be seen that the separation results are improved, which is almost consistent with the theoretical values.

These results are finally compared with those obtained by frequency-domain approach, which are shown in Figure 16. As can be seen from Figure 16, the separated regional anomaly is more flat than the theoretical one, while the separated residual anomaly contains some component of regional anomaly, if we choose the typical cut-of frequency 2/L (L is the length of profile).

Comparing Figure 15 and 16, we find that our approach can obtain better separation results than conventional frequency-domain method.

C. SEPARATION EXPERIMENT FOR THE 2D MODEL WITH NOISE

To analysis the sensitivity to noise of our approach, 10 db Gaussian white noise was added to the synthetic data of model 1 (see Figure 17 for the noisy data). The classical separation method based on MRA, frequency domain filtering method, and our approach was employed to separate the synthetic data with noise, respectively.

Figure 18 shows the wavelet coefficients of MRA of magnetic anomaly of model 1 with 10 db Gaussian white noise. From Figure 18a we can see that the coefficients in the yellow

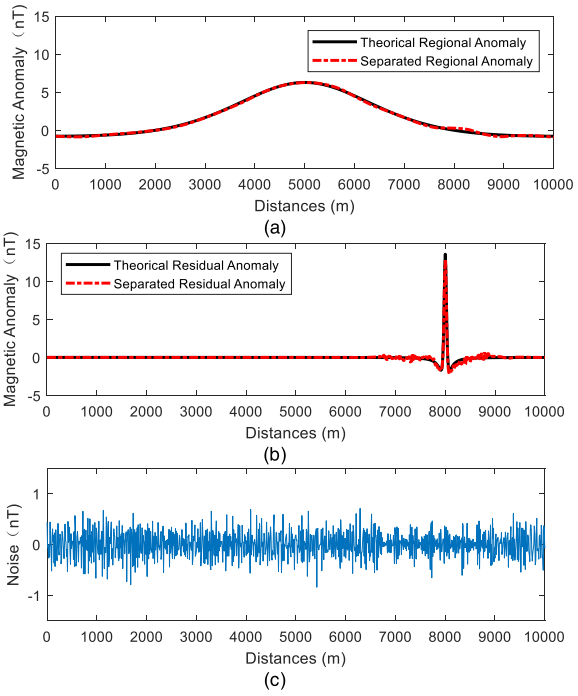

FIGURE 20. Separation result of magnetic anomaly of model 1 with spatial locating MRA and optimal mother wavelet, say 'sym5', as: (a) regional anomaly; (b) regional anomaly; (c) noise.

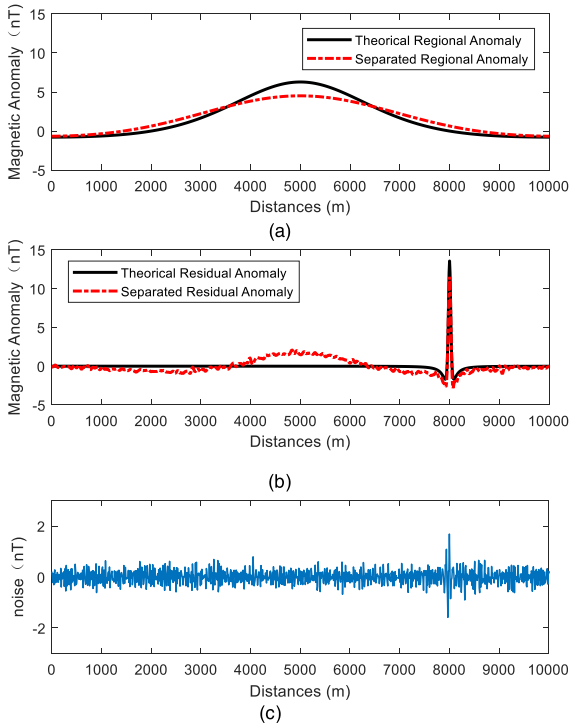

FIGURE 21. Separation result of magnetic anomaly with 10 db Gaussian white noise of model 1 of frequency filtering with 2/L and 0.13 cut-off frequency as: (a) regional anomaly; (b) residual anomaly; (c) noise.

dashed box represent the high frequency noise, the coefficients in the green dashed box represent the regional anomaly, while the coefficients in the red box represent the residual

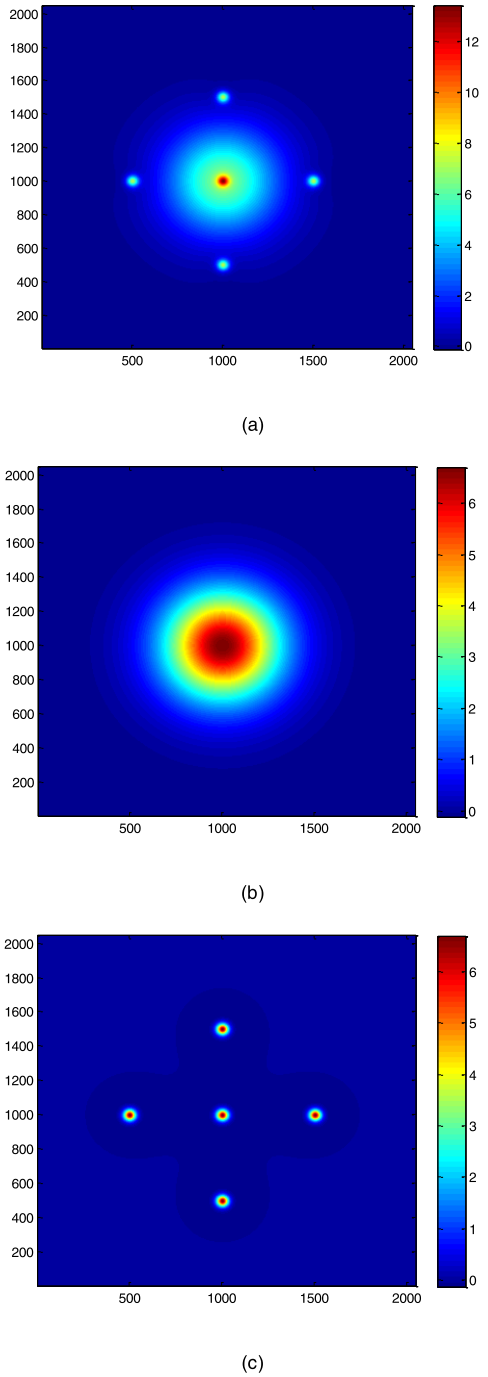

FIGURE 22. The magnetic anomaly of model 2: (a) total magnetic anomaly; (b) magnetic anomaly of big sphere (regional anomaly); (c) magnetic anomaly of five small spheres (residual anomaly).

anomaly. From Figure 18b we can see clearly that the noise and residual anomaly alias on 9^{th} detail coefficients.

According to the above analysis, the noise is reconstructed by $9^{th} - 10^{th}$ order detail coefficients, and the residual anomaly is reconstructed by $6^{th} - 8^{th}$ order detail coefficients, and the regional anomaly is reconstructed by the rest coefficients. The separation results are shown in Figure 19.

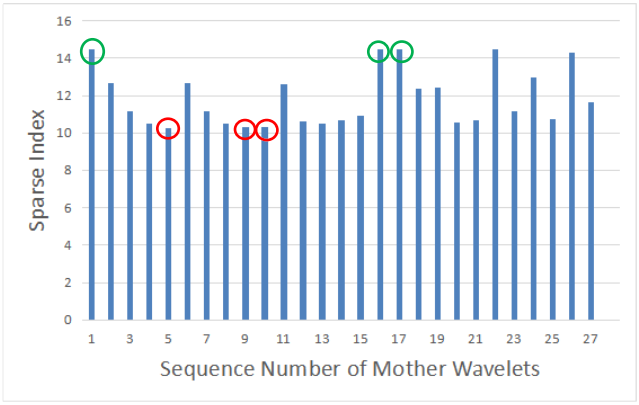

FIGURE 23. The factor SI of the magnetic anomaly of model 2 using different mother wavelets.

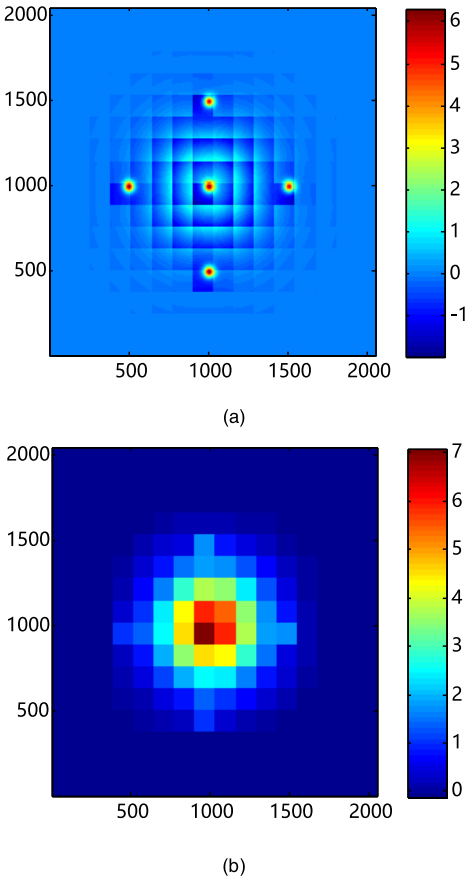

FIGURE 24. Separation result of magnetic anomalies of model 2 with worst mother wavelet 'db1' as: (a) separated residual anomalies; (b) separated regional anomalies.

We can see, from Figure 19, that (1) the separated regional anomaly and noise contains some part of residual information, respectively (see the blue dashed box in Figure 19a, 19c). Correspondingly, the result of residual anomaly is attenuated (see the blue dashed box in Figure 19b). (2) The separated residual contains part of noise (see the green dashed box in Figure 19b).

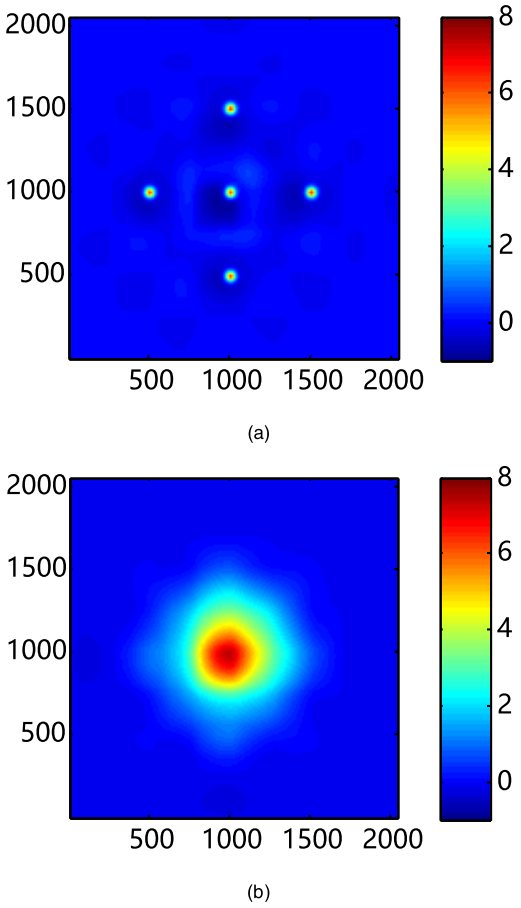

FIGURE 25. Separation result of magnetic anomaly of model 2 with optimal mother wavelet 'sym5' as: (a) separated residual anomaly; (b) separated regional anomaly.

If we utilize the spatial information of wavelet transform, we will obtain better separation results by using the coefficients in the yellow dashed box but not in red box, using the coefficients in the red box, and using the coefficients in the green dashed box but not in red box in the Figure 18a to reconstruct the noise, residual anomaly, and the regional anomaly, respectively. The separation results of our approach are shown in Figure 20.

From Figure 20 we can see that the residual and regional anomalies are separated more accurately by using our spatial locating MRA method from the noisy synthetic data. The separation results are almost consistent with the theoretical values.

These results are also compared with those obtained by frequency-domain approach, which are shown in Figure 21. As can be seen from Figure 21, the separated regional anomaly is more flat than the theoretical one, while the separated residual anomaly contains some component of regional anomaly and noise, if we choose the typical cut-of frequency 2/L (L is the length of profile).

Comparing Figure 20 and 21, we find that our approach can obtain better separation results than conventional frequency-domain method.

TABLE 3. Parameters of model 2 (3D geological bodies model of one big sphere and five small spheres).

Model	Center of sphere			Radius (m)	Magnetization (A/m)
	x (m)	y (m)	z (m)		
Big sphere	1000	1000	100	100	1
Small sphere 1	500	1000	50	10	1
Small sphere 2	1500	1000	50	10	1
Small sphere 3	1000	1000	50	10	1
Small sphere 4	1000	500	50	10	1
Small sphere 5	1000	1500	50	10	1

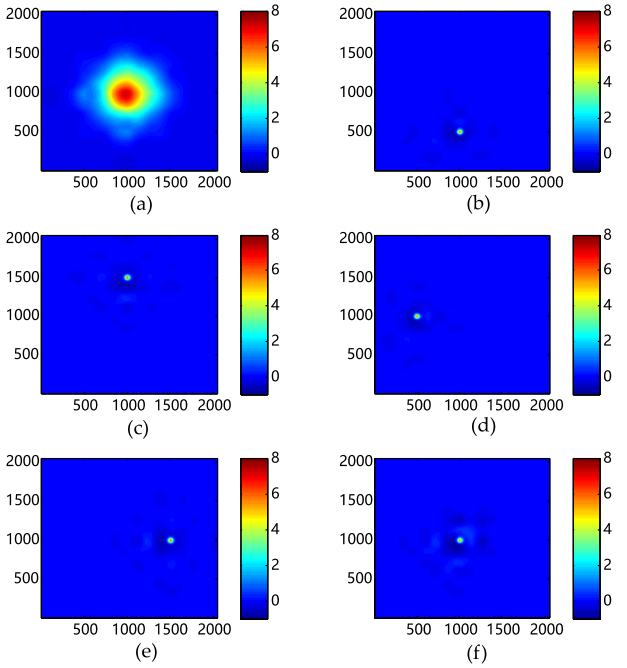

FIGURE 26. Separation result of magnetic anomaly of model 2 with spatial locating MRA and optimal mother wavelet 'sym5' as: (a) regional anomaly of big sphere; (b) residual anomaly of small sphere 1; (c) residual anomaly of small sphere 2; (d) residual anomaly of small sphere 3; (e) residual anomaly of small sphere 4; (f) residual anomaly of small sphere 5.

D. SEPARATION EXPERIMENT FOR THE 3D MODEL

Model 2: This is 3D geological bodies model which consists of a big deeper sphere and five small shallower spheres. For the big sphere, center of sphere is (1000m, 1000m, 500m), radius is 100m, magnetization is 1 A/m; For the five small spheres, center of sphere is (500m, 1000m, 50m), (1500m, 1000m, 50m), (1000m, 1000m, 50m), (1000m, 500m, 50m), (1000m, 1500m, 50m), respectively, the radius are all 10m, and the magnetization are all 1A/m. The parameters of model 2 are listed in Table 3.

The observation area on the ground is $2000m \times 2000m$, the observation interval is 10m. The observed magnetic anomaly of model 2 is shown in Figure 22.

For model 2 magnetic anomaly, a set of mother wavelets (see Table 1) are selected to calculate their corresponding SI, and the results are shown in Figure 23.

As can be seen from Figure 23, the three best mother wavelets are 'db5', 'sym5' and 'sym6' (mother wavelets numbered 5, 9 and 10 in the red circle). The three worst mother wavelets are 'db1', 'bior1.1' and 'bior1.3' (mother wavelets numbered 1, 16 and 17 in the green circle).

The worst mother wavelet 'db1' and the optimal mother wavelet 'sym5'; are employed to separate the magnetic anomaly of model 2. The separation results are shown in Figure 24 (using 'db1') and Figure 25 (using 'sym5'), respectively. Comparing the Figure 24 and 25, it can be seen that the separation results using optimal mother wavelet are much better than the worst one, which can separate the anomaly of big sphere (regional anomaly) and of five small spheres (residual anomaly) clearly.

Furthermore, we could separate the anomaly of each sphere, see in Figure 26, using spatial locating MRA separation and optimal mother wavelet. The finer separation results could help us to obtain a better geological interpretation later.

IV. CONCLUSIONS

In this work, a geophysical potential field separation method based on optimal mother wavelet and spatial locating MRA is proposed. The quantitative evaluation factor, Sparse Index (SI), is proposed to help us choosing the optimal mother wavelet for a given separation task. The Spatial locating MRA method separates the regional and residual anomaly, by means of reconstructing them using the wavelet coefficients within particular spatial and scale arrange, respectively.

The proposed separation method is evaluated on four experiments, including a 2D (without and with noise) and a 3D geological body model separation task. The results show that our approach can choose optimal mother wavelet quantitatively, and separates the geophysical potential field into regional and residual anomaly more clear then the classical MRA method and conventional frequency domain filtering method, when the spectrum of regional residual anomaly are aliased. The finer separation results are helpful for the later geological interpretation.

ACKNOWLEDGMENT

The authors would like to thank the anonymous reviewers for their constructive and helpful comments.

REFERENCES

[1] W. J. Hinze, R. R. Von Frese, R. Von Frese, and A. H. Saad, *Gravity and Magnetic Exploration: Principles, Practices, and Applications*. Cambridge, U.K.: Cambridge Univ. Press, 2013.

[2] K. Liu *et al.*, "3D gravity anomaly separation method taking into account the gravity response of the inhomogeneous mantle," *J. Asian Earth Sci.*, vol. 163, pp. 212–223, Sep. 2018.

[3] M. N. Nabighian *et al.*, "The historical development of the magnetic method in exploration," *Geophysics*, vol. 70, no. 6, pp. 33ND–61ND, 2005.

[4] C.-Y. Liu, C.-L. Yao, and Y.-M. Zhen, "Preferential spatially varying filtering method in the wavelet domain for gravity anomaly separation," *Chin. J. Geophys.*, vol. 58, no. 12, pp. 4740–4755, 2015.

[5] A. Spector and F. S. Grant, "Statistical models for interpreting aeromagnetic data," *Geophysics*, vol. 35, no. 2, pp. 293–302, Apr. 1970.
[6] R. S. Pawlowski, "Green's equivalent-layer concept in gravity band-pass filter design," *Geophysics*, vol. 59, no. 1, pp. 69–76, Jan. 1994. doi: 10.1190/1.1443535.
[7] P. Keating and N. Pinet, "Use of non-linear filtering for the regional–residual separation of potential field data," *J. Appl. Geophys.*, vol. 73, no. 4, pp. 315–322, Apr. 2011.
[8] L. Guo, X. Meng, Z. Chen, S. Li, and Y. Zheng, "Preferential filtering for gravity anomaly separation," *Comput. Geosci.*, vol. 51, pp. 247–254, Feb. 2013.
[9] P. S. Addison, "Introduction to redundancy rules: the continuous wavelet transform comes of age," *Philos. Trans. Ser. A, Math. Phys. Eng. Sci.*, vol. 376, Aug. 2018, Art. no. 20170258. [Online]. Available: doi: 10.1098/rsta.2017.0258.
[10] K. Dziedziech, A. Nowak, A. Hasse, T. Uhl, and W. J. Staszewski, "Wavelet-based analysis of time-variant adaptive structures," *Philos. Trans. Ser. A, Math. Phys. Eng. Sci.*, vol. 376, Jul. 2018, Art. no. 20170245. [Online]. Available: doi: 10.1098/rsta.2017.0245.
[11] M. Srivastava, C. L. Anderson, and J. H. Freed, "A new wavelet denoising method for selecting decomposition levels and noise thresholds," *IEEE Access*, vol. 4, pp. 3862–3877, 2016.
[12] S. G. Mallat, "A theory for multiresolution signal decomposition: The wavelet representation," *IEEE Trans. Pattern Anal. Mach. Intell.*, vol. 11, no. 7, pp. 674–693, Jul. 1989.
[13] M. Fedi and T. Quarta, "Wavelet analysis for the regional-residual and local separation of potential field anomalies," *Geophys. Prospecting*, vol. 46, no. 5, pp. 507–525, Sep. 1998. doi: 10.1046/j.1365-2478.1998.00105.x.
[14] W.-C. Yang, Z.-Q. Shi, and Z.-Z. Hou, "Discrete wavelet transform for multiple decomposition of gravity anomalies," *Chin. J. Geophys.*, vol. 44, no. 4, pp. 529–537, Jul. 2001.
[15] O. N. Ucan, A. M. Albora, and Z. M. Hisarli, "Comments on the gravity and magnetic anomalies of Saros Bay using wavelet approach," *Mar. Geophys. Res.*, vol. 22, no. 4, pp. 251–264, Jul. 2001.
[16] H. Wang, Z. Luo, J. Ning, and J. Luo, "Separation of gravity anomalies based on multiscale edges," (in Chinese), *Wuhan Daxue Xuebao, Xinxi Kexue Ban*, vol. 34, no. 1, pp. 109–112, 2009.
[17] Y. Yushan, L. Yuanyuan , and L. Tianyou, "Gravity and magnetic investigation on the distribution of volcanic rocks in the Qinggelidi area, northeastern Junggar Basin (north-west China)," *Geophys. Prospecting*, vol. 60, no. 3, pp. 539–554, 2012.
[18] Z.-Z. Hou, W.-C. Yang, and C.-Q. Yu, "Three-dimensional density structure of north China's craton crust and its geological implications," *Chin. J. Geophys.*, vol. 57, no. 4, pp. 520–531, 2014.
[19] H. Li, C.-B. Yang, Y.-G. Wu, H.-F. Huan, and T. Gao, "Application of wavelet transform for de-noising and potential field separation in gravity and magnetic data processing," *Global Geol.*, vol. 33, no. 1, pp. 200–208, 2014.
[20] I. Daubechies, *Ten Lectures on Wavelets*. Philadelphia, PA, USA: SIAM, 1992.
[21] P. S. Addison, *The Illustrated Wavelet Transform Handbook*. Bristol, U.K.: IOP Publishing Ltd, 2002.
[22] K. J. Friesen, N. Panagiotacopulos, and W. L. Sjogren, "Analysis of gravity signals and gravity potential determination using order 8 multiresolution analysis discrete wavelets," in *Proc. Adv. Phys. Electron. Signal Process. Appl. WSES Press, Athens*, Sep. 2000, pp. 303–308.
[23] W. K. Ngui, M. S. Leong, L. M. Hee, and A. M. Abdelrhman, "Wavelet analysis: Mother wavelet selection methods," *Appl. Mech. Mater.*, vol. 393, pp. 953–958, Sep. 2013.
[24] M. Ibrahim *et al.*, "Selection of mother wavelet and decomposition level for energy management in electrical vehicles including a fuel cell," *Int. J. Hydrogen Energy*, vol. 40, no. 45, pp. 15823–15833, Dec. 2015.

CAI-YUN LIU received the B.S. degree in applied mathematics from the Huazhong University of Science and Technology, China, in 1998, the M.S. degree in applied mathematics from Yangtze University, China, in 2008, and the Ph.D. degree in geophysics and information technology from the China University of Geosciences, China, in 2014. She is currently an Associate Professor with the School of Information and Mathematics, Yangtze University. Her research interests include geophysical data processing, wavelet analysis, gravity and magnetic exploration, and applied mathematics.

CHANG-LI YAO received the B.S. degree in geophysical exploration from Hefei Polytechnic University, China, in 1988, and the M.S. degree in applied geophysics and the Ph.D. degree in geophysics and information technology from the China University of Geosciences, China, in 1991 and 2002, respectively, where he is currently a Professor with the School of Geophysics and Information Technology. His research interests include gravity and magnetic exploration, computer application, and geomagnetism.

JIE XIONG received the B.S. degree in computer communication from the Chongqing University of Posts and Telecommunications, China, in 1998, the M.S. degree in computer science from Yangtze University, China, in 2005, and the Ph.D. degree in geophysics and information technology from the China University of Geosciences, China, in 2012. He is currently an Associate Professor with the School of Electronics and Information, Yangtze University. His research interests include computer application, applied geophysics, and artificial intelligence.